A Lagrangian Framework to Incorporate Positional and Velocity Constraints to Achieve Path-Following Control

Ehsan Peymani

Thor I. Fossen

Abstract—In this paper, inspired by Lagrangian mechanics, a marine craft is regarded as a mechanical system subject to both holonomic and nonholonomic constraints. Then, the forces that secure fulfilment of the constraints are derived. The proposed method is used to design a controller which makes the craft converge to straight-line paths with an exponential rate. A method to handle underactuation in sway is also proposed. Simulation results demonstrate the performance of the proposed method, and enlighten the effect of the new selection of constraints for the path-following problem.

I. INTRODUCTION

In many applications, a marine craft has to move along a given path. Compared to trajectory tracking (TT) [1] in which a vehicle is forced to track pre-specified time functions of all states, path following (PF) removes temporal constraints and reduces the tracking problem to only a subset of states. In [2], the authors highlight an underlying difference between TT and PF for non-minimum-phase systems. In addition, the stability proof of the full-state TT [3] needs yaw velocity to be persistently exciting, indicating that straight paths cannot be tracked. The shortest path between any two poses can always be characterized by a combination of at most two curves and one straight line [4]. Moreover, in maritime applications, routes are usually expressed in terms of waypoints [5] and made up of straight segments. This motivates methods for straight-line path following.

Many marine craft are underactuated; thus, for practical purposes, underactuation must be taken into account. Control of underactuated craft is challenging. According to [6] and [7], underactuation may place a nonholonomic constraint at the acceleration level and causes difficulties for classical control methods, see [8] for more details.

Path following of underactuated ships have been investigated in many papers. Most of works for straight-line PF are guidance-based and use the line-of-sight (LOS) guidance method. References [9]–[11] present control methods for straight-line PF and waypoint tracking that put a lower bound on the LOS lookahead distance to render the cross-track error and sway velocity uniformly globally asymptotically stable (UGAS) at the origin. In [12], a robust and adaptive controller using backstepping method is developed, which discusses the LOS lookahead distance for boundedness of the unactuated dynamics in the presence of external disturbances. Based on the backstepping technique, [13] proposes a controller

that forces the heading to follow the desired heading while stabilizing forward speed. To deal with underactuation, it assigns dynamics to the stabilizing function, and propose a dynamic controller. Robustification of the method is carried out with constant parameter adaptation in [14]. However, neither analyzes convergence to the desired path.

In [15], a method for formation control of a fleet of fully actuated marine surface craft is put forward. The idea is to conceive the control objectives as mechanical constraints and treat the system as a constrained system. Then, the Lagrange multiplier method is employed to derive the forces that secure fulfillment of the constraints. This method deals *only* with holonomic constraints which place restriction on position variables. However, in some applications, it is required to assign desired values to velocity variables, which imposes nonholonomic constraints on the system.

The main contribution of the paper is twofold. First, a systematic approach to simultaneously handle both positional and velocity constraints is proposed in order to solve various motion control schemes e.g. PF and formation control. More precisely, the paper generalizes the recent paper [15] to strategies that include speed assignments.

Second, we aim to show how new constraints can be included in path following problems and how well it results. Indeed, the proposed method provides an approach that facilitates inclusion of new constraints. As a consequence, in contrast to the previous above-mentioned works, the cross-track error can be proved uniformly globally exponentially stable (UGES) regardless of the guidance system parameter. The controller is in a generic setting so as to have the capability to control both fully actuated and underactuated marine craft.

After introduction, a brief review of Lagrangian mechanics dealing with constrained systems is presented. In Section III, the problem is formulated. Section IV is devoted to the proposed control method and summarizes the main result of the paper. The controller is demonstrated using computer simulations. The paper ends with conclusion.

II. LAGRANGIAN MECHANICS FOR CONSTRAINED MOTION

The Lagrangian of a mechanical system [16] in an n-dimensional configuration space, uniquely described using a set of generalized coordinates $\boldsymbol{q}$, is defined as

$$\mathcal{L}(\boldsymbol{q}, \dot{\boldsymbol{q}}) \triangleq \mathcal{T}(\boldsymbol{q}, \dot{\boldsymbol{q}}) - \mathcal{V}(\boldsymbol{q}) \tag{1}$$

in which $\mathcal{T} = \frac{1}{2}\dot{\boldsymbol{q}}^T \mathcal{M}(\boldsymbol{q})\dot{\boldsymbol{q}}$ is the kinetic energy, $\mathcal{V}(\boldsymbol{q})$ is the potential energy, and the matrix $\mathcal{M}(\boldsymbol{q}) \in \mathbb{R}^{n \times n}$ is the mass

and inertia matrix. The vector $\dot{q}$ is the vector of generalized velocities. The Lagrange-D'Alembert principle states how the Lagrangian of a mechanical system exposed to the generalized forces τ connects with the equations of motion:

$$\frac{d}{dt}\frac{\partial \mathcal{L}}{\partial \dot{q}_i} - \frac{\partial \mathcal{L}}{\partial q_i} = \tau_i, \qquad i = 1, \cdots, n \tag{2}$$

which are also known as the Euler-Lagrange equations. Equation (2) results in

$$\mathcal{M}(q)\ddot{q} + n(q,\dot{q}) = \tau \tag{3}$$

$$\text{where} \quad n(q,\dot{q}) = \left(\dot{\mathcal{M}}(q) - \frac{1}{2}\dot{q}^T\frac{\partial \mathcal{M}(q)}{\partial q}\right)\dot{q} + \frac{\partial \mathcal{V}(q)}{\partial q}$$

The Lagrangian mechanics deals with constrained systems in an appealing way that is discussed in the following.

A. Holonomic Constraints

A system can be subject to k geometric constraints:

$$G(q,t) = 0 \tag{4}$$

which are defined on generalized coordinates and usually called holonomic constraints. They may arise when one part of the body must be in contact with a specific manifold. Holonomic constraints are well-defined to be tackled with Hamilton's generalized principle which augments the Lagrangian (1) with the constraints according to

$$\mathcal{L}^* = \mathcal{L} + \lambda_G^T G \tag{5}$$

This is done by introducing the Lagrange multipliers $\lambda_G \in \mathbb{R}^k$. The Euler-Lagrange equations are then applied to the augmented Lagrangian (5) over the extended set of the independent coordinates $\{q, \lambda_G\}$. This leads to the equations of motion (3) where the generalized force vector changes to

$$\tau = \tau_{ext} + \tau_c \tag{6}$$

In (6), τ_{ext} denotes the external forces and τ_c represents the forces of constraints which are given by

$$\tau_c = -\left(\frac{\partial G}{\partial q}\right)^T \lambda_G \tag{7}$$

This is referred to as the *Lagrange multiplier* method. Just bear in mind that it is presumed $G = 0$ for all t.

B. Nonholonomic Constraints

In addition to geometric constraints, a system may involve m kinematic constraints. First-order kinematic constraints can be represented by

$$K(q,\dot{q},t) = 0 \tag{8}$$

If the constraints (8) are integrable, they can be represented as an algebraic equation consisting of position variables; that is, they are in essence holonomic. Otherwise, they are said to be nonholonomic. D'Alembert's principle and any principles based on virtual displacement cannot be applied for general nonholonomic constraints [17].

For vehicles including marine craft, kinematic constraints usually are linear in velocity

$$\mathcal{A}(q,t)\dot{q} + \mathcal{B}(q,t) = 0 \tag{9}$$

If the constraint set (9) is driftless and does not explicitly depend on time, it is called *Pfaffian*. In the case of integrability of (9), they can be integrated and represented as the geometric constraints (4). The constraints are then termed *semi-holonomic*. Such constraints can be treated as holonomic constraints with the Lagrange multiplier method developed from D'Alembert's generalized principle even though the integrated form is not known.

However, if the constraints (9) are not integrable, they are nonholonomic. In this case, augmentation of the Lagrangian akin to what is carried out for holonomic constraints is not correct. The proper principle to apply is D'Alembert's *basic* principle [17] which results in the fact that a system with the equations of motion (3) subject to nonholonomic constraints (9) is enforced by the vector τ in the form (6) but τ_c is computed using

$$\tau_c = -\mathcal{A}^T \lambda_K, \qquad \lambda_K \in \mathbb{R}^m \tag{10}$$

C. Systems subject to both constraints

If a system is subject to m nonholonomic constraints C_1, linear in velocity, and k holonomic constraints C_2, the constraint force vector τ_c is computed using [18]

$$\tau_c = -\mathcal{W}^T \lambda \tag{11}$$

in which $\mathcal{W} \triangleq [\mathcal{W}_1^T, \mathcal{W}_2^T]^T$, is called the *Jacobian matrix*, where

$$\mathcal{W}_1 = \partial C_1/\partial \dot{q}, \qquad \mathcal{W}_2 = \partial C_2/\partial q \tag{12}$$

and $\lambda \triangleq [\lambda_1^T, \lambda_2^T]^T$ with $\lambda_1 \in \mathbb{R}^m$ and $\lambda_2 \in \mathbb{R}^k$.

III. PROBLEM FORMULATION

This paper addresses the problem of path maneuvering to straight-line paths which involves a LOS guidance system and a nonlinear controller. The maneuvering problem is divided into two subproblems [19]:

1) *Geometric* task which is to reduce the distance between the vehicle and the path. The LOS guidance system is in charge of mapping the desired position (x_d, y_d) into the desired heading ψ_d. This objective is primary and imposes holonomic constraints on the system.
2) *Dynamic* task which is to make the forward velocity track the desired speed profile, u_d. This objective is of secondary importance as moving on the path is more important than moving with the desired speed. It places nonholonomic constraints on the system.

A. Line-of-Sight (LOS) Guidance System

Here, the LOS projection algorithm, taken from [5], is presented. It is assumed that the path is characterized using a predefined set of waypoints, and it is composed of straight-line segments connecting any two successive waypoints. The aim of the guidance system is to compute the desired heading

ψ_d that the vehicle has to acquire in order for moving toward the path and after reaching the path, moving along it.

Assume that the waypoints are denoted by $\boldsymbol{p}_i = [x_i, y_i]^T$ and two active points are indexed by k and $k+1$. The slope of the straight line connecting them is denoted by α_k. The cross-track error, defined as the shortest distance between the vehicle and the path, is found using

$$e(t) = -(x - x_k)\sin(\alpha_k) + (y - y_k)\cos(\alpha_k) \quad (13)$$

where x and y represent the current position of the vehicle. The desired heading angle is then given by

$$\psi_d(t) = \operatorname{atan2}(-e/\Delta) \in (-\pi, \pi) \quad (14)$$

$\Delta > 0$ is called the *lookahead distance*, which specifies the point ahead of the ship along the path toward which the ship is asked to move.

A simple switching criterion is employed to select the active waypoints. If the along-track error between the vehicle and waypoint $\boldsymbol{p}_k$ is

$$s(t) = (x - x_k)\cos(\alpha_k) + (y - y_k)\sin(\alpha_k) \quad (15)$$

and the along-track error between two active waypoints is denoted by s_k, the active waypoints will be $k+1$ and $k+2$ if $s(t) - s_k > L$ where L is a predefined threshold. According to [5], this is the lookahead-based steering method which aligns the x-axis of $\{b\}$ with LOS vector.

B. Standard Model of Surface Marine Craft

A standard model for marine surface craft is considered [5]. The position and the heading of the vessel expressed in the inertial frame $\{i\}$ is represented by $\boldsymbol{\eta} = [x, y, \psi]^T \in \mathbb{R}^2 \times \mathcal{S}^1$. The body-fixed velocities are given by $\boldsymbol{\nu} = [u, v, r]^T \in \mathbb{R}^3$ which are related to the generalized velocities through the kinematics

$$\dot{\boldsymbol{\eta}} = \mathcal{R}(\psi)\boldsymbol{\nu} \quad (16)$$

where the rotation matrix $\mathcal{R}(\psi)$ is

$$\mathcal{R}(\psi) = \begin{bmatrix} \cos(\psi) & -\sin(\psi) & 0 \\ \sin(\psi) & \cos(\psi) & 0 \\ 0 & 0 & 1 \end{bmatrix} \quad (17)$$

The kinetics is described by

$$\mathcal{M}_b\dot{\boldsymbol{\nu}} + \mathcal{C}_b(\boldsymbol{\nu})\boldsymbol{\nu} + \mathcal{D}_b(\boldsymbol{\nu})\boldsymbol{\nu} = \boldsymbol{\tau}_p^b + \boldsymbol{\tau}_c^b \quad (18)$$

where $\boldsymbol{\tau}_p^b$ denotes the actuator force vector expressed in body-fixed frame $\{b\}$, and $\boldsymbol{\tau}_c^b = \mathcal{R}^T(\psi)\boldsymbol{\tau}_c$ represents the constraint forces (11) transformed from $\{i\}$ to $\{b\}$. In (18), $\mathcal{M}_b = \mathcal{M}_b^T > 0$, $\dot{\mathcal{M}}_b = 0$ is the mass and inertia matrix, $\mathcal{C}_b(\boldsymbol{\nu})$ is the Coriolis and centripetal matrix and $\mathcal{D}_b(\boldsymbol{\nu})\boldsymbol{\nu}$ captures damping forces. They take the following forms:

$$\mathcal{M}_b = \begin{bmatrix} m_{11} & 0 & 0 \\ 0 & m_{22} & m_{23} \\ 0 & m_{23} & m_{33} \end{bmatrix}, \mathcal{D}_b = \begin{bmatrix} d_{11} & 0 & 0 \\ 0 & d_{22} & d_{23} \\ 0 & d_{23} & d_{33} \end{bmatrix}$$

$$\mathcal{C}_b = \begin{bmatrix} 0 & 0 & -(m_{22}v + m_{23}r) \\ 0 & 0 & m_{11}u \\ m_{22}v + m_{23}r & -m_{11}u & 0 \end{bmatrix}$$
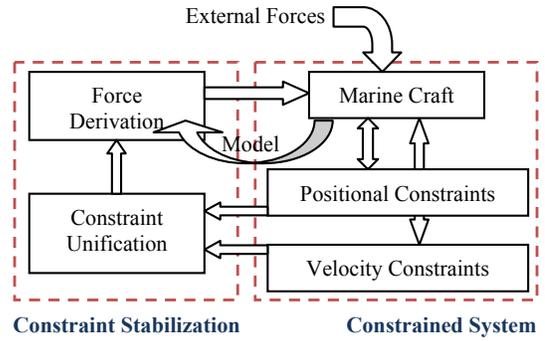

Fig. 1: Diagram of the proposed framework.

Note that surge is decoupled from sway and yaw due to symmetry assumption in xz-plane. Kinetics (18) can be represented in terms of the generalized coordinates and velocities using (16). In this case, it takes the form of (3) with

$$\mathcal{M}(\boldsymbol{\eta}) = \mathcal{R}(\psi)\mathcal{M}_b\mathcal{R}(\psi)^T$$

$$\boldsymbol{n} = \mathcal{R}(\psi)\left(\mathcal{C}_b(\boldsymbol{\nu})\boldsymbol{\nu} + \mathcal{D}_b(\boldsymbol{\nu})\boldsymbol{\nu} - \mathcal{M}_b\mathcal{R}^T\dot{\mathcal{R}}\right)\mathcal{R}(\psi)^T$$

In the case of underactuation, $\tau_v = 0$; i.e. $\boldsymbol{\tau} = [\tau_u, 0, \tau_r]^T$.

C. Control Objectives and Constraint Functions

Mathematically, the control objectives are defined here. Assume that $u_d(t) > 0$, and $u_d \in \mathcal{C}^1$. The first objective is

$$\lim_{t\to\infty} \tilde{u} = 0, \qquad \text{where } \tilde{u}(t) \triangleq u(t) - u_d(t) \quad (19)$$

In addition, we want to make $\tilde{\psi}(t) \triangleq \psi(t) - \psi_d(t)$ converge to zero while the ship approaches the path; equivalently, the objectives are:

$$\lim_{t\to\infty} \tilde{\psi}(t) = 0 \quad \text{and} \quad \lim_{t\to\infty} e(t) = 0 \quad (20)$$

Therefore, one can place these constraints on the system

$$\boldsymbol{C}_1 = \begin{bmatrix} \cos(\psi) & -\sin(\psi) \\ \sin(\psi) & \cos(\psi) \end{bmatrix} \begin{bmatrix} \dot{x} \\ \dot{y} \end{bmatrix} - \begin{bmatrix} u_d \\ v_d \end{bmatrix} \equiv \mathcal{W}_1(\boldsymbol{\eta})\dot{\boldsymbol{\eta}} + \boldsymbol{\alpha}_1(t)$$
$$\quad (21)$$

$$\boldsymbol{C}_2 = \begin{bmatrix} \psi - \psi_d(t) \\ e \end{bmatrix} \quad (22)$$

which implies that $\boldsymbol{C}_1$ is nonholonomic and $\boldsymbol{C}_2$ is holonomic. The second element of $\boldsymbol{C}_1$ is equivalent to $\tilde{v} \triangleq v - v_d$. If the vessel is fully actuated, v_d can be set equal to zero to avoid moving sideways. In the case of underactuation, as it will be discussed later, it introduces a differential equation that ensures boundedness of the unactuated dynamics and assures internal stability of the closed-loop system.

D. Framework Overview

A schematic diagram of the constrained control framework is displayed in Fig. 1. Actually, the velocity and position of the system described by (16) and (18) are restricted to the manifolds described by the constraints (21) and (22). Hence, the constraint forces are computed such that the constraints are always fulfilled; that is, $\boldsymbol{C}_1 = 0$ and $\boldsymbol{C}_2 = 0$. The following section explains the constraint stabilization block in Fig. 1.

IV. CONSTRAINT STABILIZATION: CONTROL DESIGN

In this section, a method that makes the ship converge to a single straight-line segment is proposed. For simplicity, the inertial frame is rotated such that the x-axis becomes tangent to the path. Accordingly, $\alpha_k = 0$ and $e = y - y_k$.

Recalling the requirement, stated in III-C, that $C_2 = 0$ has to hold always, C_2 is stabilized using

$$\dot{C}_2 + \mathcal{K}_2 C_2 = 0 \Rightarrow \mathcal{W}_2 \dot{\eta} + \alpha_2(t) + \mathcal{K}_2 C_2 = 0 \qquad (23)$$

in which $\mathcal{K}_2 = \text{diag}(k_1, k_2) > 0$ and $\alpha_2 = [-\dot{\psi}_d, 0]^T$. Noting the definitions of the Jacobian matrixes in (12) and the expression of C_1, (21) and (23) are lumped together, which results in the *unified constraint*:

$$\Phi = \mathcal{W} \dot{\eta} + a(\eta, t) \qquad (24)$$

in which $a(\eta, t) = [\alpha_1, \alpha_2 + \mathcal{K}_2 C_2]^T$ and $\alpha_1 = -[u_d, v_d]^T$. According to (21)-(22), we have

$$\mathcal{W} = \left[\begin{array}{cc} \mathcal{R}(\psi)^T & \\ 0 \quad 1 \quad 0 \end{array} \right] \qquad (25)$$

It is required to stabilize the unified constraints (24) to be sure that (21) and (23) are satisfied. This is done using a *P*-type controller:

$$\dot{\Phi} + \mathcal{K}_\Phi \Phi = 0$$
$$\Rightarrow \mathcal{W}(\eta) \ddot{\eta} + \dot{\mathcal{W}}(\eta) \dot{\eta} + \dot{a}(\eta, t) + \mathcal{K}_\Phi \Phi = 0 \quad (26)$$

in which $\mathcal{K}_\Phi = \text{diag}\{k_u, k_v, k_3, k_4\} > 0$. Solving (3) for $\ddot{\eta}$ and substituting the solution in (26), an algebraic equation for the multipliers λ is developed

$$\mathcal{W} \mathcal{M}^{-1} \mathcal{W}^T \lambda = -\mathcal{W} \mathcal{M}^{-1} n + \dot{\mathcal{W}} \dot{\eta} + \dot{a} + \mathcal{K}_\Phi \Phi \qquad (27)$$

Using (11), the constraint forces are computed as

$$\tau_c = -\mathcal{M} \mathcal{W}^\dagger \left(\dot{\mathcal{W}} \dot{\eta} + \dot{a} + \mathcal{K}_\Phi \Phi \right) + n \qquad (28)$$

in which $\mathcal{W}^\dagger$ is the Moore–Penrose pseudo–inverse, which is given by $\mathcal{W}^\dagger = \left(\mathcal{W}^T \mathcal{W} \right)^{-1} \mathcal{W}^T$.

The control problem is solvable if the inversion is possible. Strictly speaking, the constraint set must include neither conflicting nor redundant constraints. For the current choice of constraints, there is no singularity, as $\det(\mathcal{W}^T \mathcal{W}) = 2$.

It is valuable to highlight that $\mathcal{W}$ acts like a transformation matrix to translate λ defined in a 4-D configuration space into τ defined in a 3-D workspace. Since we need to apply the forces to the system, the forces are directly derived. For the current problem, $\mathcal{W}^\dagger$ is equal to

$$\underbrace{\left[\begin{array}{cc} & 0 \\ \mathcal{R}(\psi) & 0 \\ & 0 \end{array} \right]}_{\mathcal{R}_n} - \frac{1}{2} \underbrace{\left[\begin{array}{cccc} 0 & 0 & 0 & 0 \\ \sin(\psi) & \cos(\psi) & 0 & -1 \\ 0 & 0 & 0 & 0 \end{array} \right]}_{\mathcal{R}_e} \qquad (29)$$

Eq. (29) suggests decomposing the constraint forces into two parts; hence, expressing (28) in $\{b\}$, it follows that

$$\tau_c^b = \tau_n + \tau_e \qquad (30)$$

τ_n, which is the required force to make $\tilde{u}$, $\tilde{v}$, and $\tilde{\psi}$ converge to zero, is given by

$$\tau_n = n - \mathcal{M} \Omega \left(\dot{a} + \mathcal{K}_\Phi \Phi \right) \qquad (31)$$

in which $\Omega = [I_{3\times3}, 0_{3\times1}]$. Indeed, (31) is the control force that linearizes the system. The second part, τ_e is

$$\tau_e = -\mathcal{M} \mathcal{R}(\psi)^T \mathcal{R}_e(\psi) \left(\dot{\mathcal{W}} \dot{\eta} + \dot{a} + \mathcal{K}_\Phi \Phi \right) \qquad (32)$$

τ_e is developed from inclusion of the cross-track error in the design and is to guarantee exponential convergence to the path.

Remark 1. In many articles for linear course control such as [9]–[14] either convergence to the path is secured based on the lookahead distance or it is not discussed. They do not consider the cross-track error directly in the design procedure. However, in the proposed method, the cross-track error is explicitly incorporated in the design procedure, and as it follows from Theorem 1 and Corollary 2, it decays exponentially with no restrictions on the guidance system. We will discuss how it affects the speed assignment task in section V where comparison with a conventional controllers is made.

If the ship is fully actuated, one can set $v_d = 0$ and the control law (30) secures fulfillment of the control objectives (22)-(21). Defining the error system $\zeta \triangleq [\tilde{u}, \tilde{v}, \tilde{\psi}, \dot{\tilde{\psi}}, e, \dot{e}]^T$, Theorem 1 summarizes the outcome.

Theorem 1 (Fully actuated marine craft)**.** *Provided* $u_d > 0$ *and belong to* $\mathcal{C}^1$, $v_d = 0$ *and* ψ_d *is computed using* (14), *the control law* (28) *renders the error system* ζ *globally exponentially stable (GES) at the origin.*

Proof: The proof is given in Appendix A. ∎

Corollary 1. $\dot{\psi}_d$ *and* $\ddot{\psi}_d$ *exist and are globally bounded.*

Proof: It follows from Theorem 1 that $\ddot{e} + k_7 \dot{e} + k_8 e = 0$ where k_7 & k_8 are defined in the next section. Thus, e, $\dot{e}$, & $\ddot{e}$ are globally bounded. On the other hand, one can differentiate (14) w.r.t time to find an upper bound for $\dot{\psi}_d$ & $\ddot{\psi}_d$. It gives

$$\left| \dot{\psi}_d \right| \le |\dot{e}|/\Delta, \qquad \left| \ddot{\psi}_d \right| \le |\ddot{e}|/\Delta + 2|\dot{e}e|/\Delta^2 \qquad (33)$$

The inequalities (33) are globally bounded. ∎

Extension to Underactuated Marine Craft

In case the craft is not actuated in sway, the second element of (30) must be zero since it cannot be applied to the system; i.e. $\tau_{c,2}^b = 0$. $v_d(t)$ is then taken as a DOF to satisfy the new constraint prescribed by underactuation. In this regard, $\tau_{c,1}^b$ and $\tau_{c,3}^b$ depend on v_d. Consequently, the requirement is to assign a proper value to v_d such that the closed-loop control system is internally stable and the unactuated dynamics is globally bounded. Setting $\tau_{c,2}^b = 0$ and defining $k_5 = k_1 + k_3$, $k_6 = k_3 k_1$, $k_7 = k_2 + k_4$, and $k_8 = k_4 k_2$, the following differential equation emerges:

$$\left(1 - 0.5 \cos^2(\psi) \right) \dot{v}_d + d_{22} v_d + h(v_d, \zeta, t) = 0 \qquad (34)$$

Corollary 2 states the result formally.

Corollary 2 (Underactuated marine craft). *For positive $u_d \in \mathcal{C}^1$ and ψ_d given by (14), if v_d is found by integration of (34), $\tau_{c,1}^b$ and $\tau_{c,3}^b$ make the craft converge to the path exponentially fast while the forward velocity converges to the desired velocity with an exponential rate. Also, the unactuated dynamics v and the control forces are globally bounded.*

Proof: The proof is given in Appendix B. ∎

V. Simulation Study

A model of Cyber Ship II, which is a 1:70 scale model of a supply ship, is chosen to demonstrate the performance of the proposed controller for waypoint tracking in calm water. The kinematics and kinetics of the system are given by (16)-(18), and the parameters are selected as:

$$m_{11} = 22.8 \quad m_{22} = 33.8 \quad m_{23} = m_{32} = 1.01 \quad m_{33} = 2.7$$
$$d_{11} = 2 \quad d_{22} = 7 \quad d_{23} = d_{32} = 0.10 \quad d_{33} = 0.5$$

The model includes the Coriolis and centripetal matrix as expressed in III-B. The ship is unactuated in sway. The desired forward speed is $u_d = 0.1$ m/s. The maximum surge force and the yaw moment are 2N and 1.5Nm, respectively. Saturation blocks are placed in the simulation model, and the controller gains are picked so as to avoid saturation while reasonable growth rate of forces and acceptable performance are achieved. A series of waypoints forms the path. The lookahead distance is selected as $\Delta = 3$m, which is almost twice bigger than the length of the ship, 1.3m. The threshold for switching logic (L) is 0.35m. The controller parameters are chosen $k_u = 30$, $k_v = 10$, $k_1 = k_3 = 1$ and $k_2 = k_4 = 2$. The ship is initially at rest. We compare two controllers, one of which, resembling conventional controllers, has only three constraints on surge, sway, and yaw whereas the other one has four constraints including the cross-track error. The simulation results are shown in Fig. 2.

Discussion

To derive the two controllers, the same approach is used; for each controller, the corresponding constraint functions and Jacobian matrixes are taken into consideration and the dynamics describing v_d is then developed. Therefore, the only difference between them is due to inclusion of the cross-track error. Fig. 2 shows that the controller with four constraints outperforms. In fact, the geometric task, which is the primary goal in this scenario, is better achieved when the cross-track error is included in the design procedure. Figs. 2 also reveals what happens that results in a better performance. Actually, the four-constraint controller takes the advantage of the forward speed to reduce the distance while the other always guarantees a constant speed for the craft. The fourth constraint causes an increase in forward speed when the vessel is off the path. This is the discrepancy between the proposed method and many articles in the field of waypoint tracking of marine surface vehicles. Fig. 2b also displays that the sway velocity is bounded and approaches zero for straight paths as expected. Incorporation of e results in a quicker action in yaw dynamics
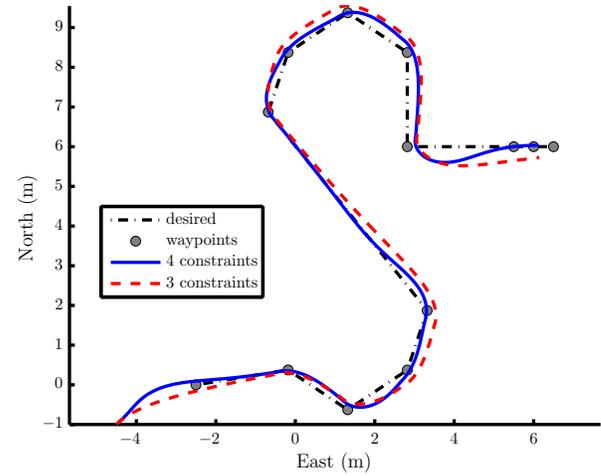
(a) The paths traveled by the ships
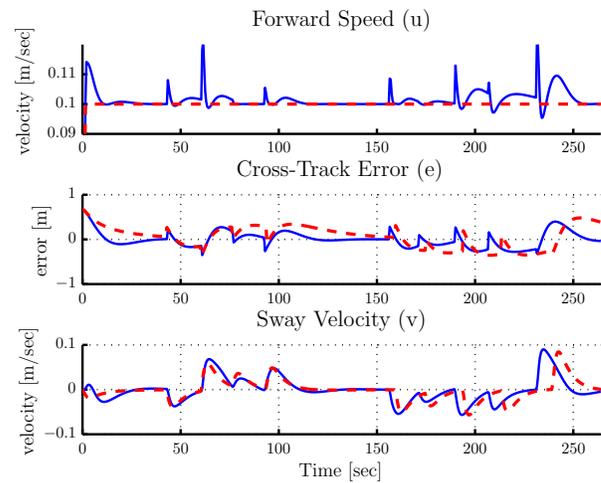
(b) forward velocity, cross-track error, and sway velocity
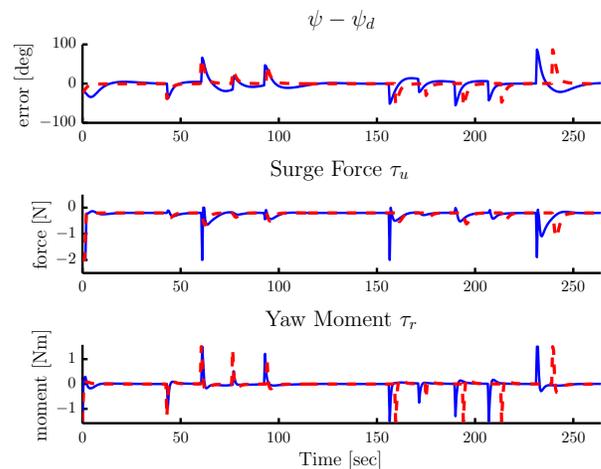
(c) Heading error along with control forces

Fig. 2: The effect of inclusion of e in the design procedure. Solid blue lines belong to the case that includes e explicitly.

(see Fig. 2c). Fig. 2c shows the control signals are well-behaved. Incorporating e may lead to reverse thrust, which

may not be practical in some cases. To avoid this, the speed controller has to have high gains.

VI. CONCLUSION

The paper successfully exploits the explicit structure of the Lagrangian formulation to develop a systematic method that handles both positional and velocity constraints for motion control of marine craft. It also demonstrates how a path-maneuvering controller that guarantees exponential convergence to a straight-line path can be designed. The prominent performance of the controller may be perceived at turning points where the controller takes the advantage of the forward speed to move towards the path as fast as an exponential function. Therefore, the proposed controller can be used in missions in which accurate path following is crucial and the speed assignment task can be sacrificed.

APENDIX A: PROOF OF THEOREM 1

Taking $V = 0.5\boldsymbol{\Phi}^T\boldsymbol{\Phi} + 0.5\boldsymbol{C}_2^T\boldsymbol{C}_2 > 0$ as the Lyapunov function, and differentiating along the solutions of (23) and (26), we get $\dot{V} = -\boldsymbol{\Phi}^T\mathcal{K}_\Phi\boldsymbol{\Phi} - \boldsymbol{C}_2^T\mathcal{K}_2\boldsymbol{C}_2 < 0$ proving that $(\boldsymbol{C}_2, \boldsymbol{\Phi}) = 0$ is GES. Then, $\tilde{\psi}, e, \tilde{u}, \tilde{v}, \dot{\tilde{\psi}} + k_1\tilde{\psi}$, and $\dot{e} + k_2 e$ are GES at the origin; so are $\dot{\tilde{\psi}}$ and $\dot{e}$.

APENDIX B: PROOF OF COROLLARY 2

It follows from Theorem 1 that $\boldsymbol{\zeta}$ is GES and globally bounded but $\boldsymbol{\tau}_c^b$ depends on v_d and $\tau_{c,2}^b = 0$. As $\tilde{v} = 0$ is GES, $\lim_{t\to\infty} v(t) = v_d(t)$ exponentially fast. The rest of the proof is devoted to demonstrate global boundedness of v_d. The function $\sigma = 0.5v_d^2 > 0$ is considered and differentiated w.r.t time. Then, an upper bound for $\dot{\sigma}$ is found using (34) and the fact that the term $(1 - 1/2\cos^2(\psi))$ belongs to $[0.5, 1]$

$$\dot{\sigma} \le -\frac{2n_{22}}{m_{22}}\sigma + |\dot{\psi}_d + \dot{\tilde{\psi}}|\sigma + \Gamma_1(|\boldsymbol{\zeta}|, t)\sqrt{2\sigma} + \Gamma_2(t)\sqrt{2\sigma} \quad (35)$$

where $\Gamma_2(t) = 0.5|\dot{u}_d|$ is uniformly globally bounded (UGB) because $\dot{u}_d$ is UGB. $m_{22}\Gamma_1(|\boldsymbol{\zeta}|, t) = \boldsymbol{W}^T|\boldsymbol{\zeta}|$ where $\boldsymbol{W}^T = [0.5m_{22}k_u + (m_{22}+2m_{11})|\dot{\psi}_d|, m_{22}k_v + 0.5m_{22}|\dot{\psi}_d| + 2d_{22} + 2m_{22}k_v, 2m_{23}k_6, (m_{22}+2m_{11})|u| + 0.5m_{22}|\tilde{v}| + 2d_{23} + 2m_{23}k_5, m_{22}k_8 + 2m_{23}k_8/\Delta, m_{22}k_7 + ((m_{22}+2m_{11})|u_d| + 2d_{23} + 2m_{23}k_7)/\Delta + 4m_{23}|e\dot{e}|/\Delta^3]$

To remove the nonlinearity in (35), the inequality $\sqrt{2\sigma} \le 1 + 2\sigma$ is used; it results in

$$\dot{\sigma} \le -\frac{2d_{22}}{m_{22}}\sigma + (|\dot{\psi}_d + \dot{\tilde{\psi}}| + 2\Gamma_1 + 2\Gamma_2)\sigma + \Gamma_1 + \Gamma_2 \quad (36)$$

To apply the comparison lemma, the corresponding equality (comparison system) for (36) is chosen as

$$\dot{\delta} = -\frac{2d_{22}}{m_{22}}\delta + g(t, \delta, \boldsymbol{\zeta}) + u_\delta(t) \quad (37)$$

in which $u_\delta(t) = \Gamma_2(t)$ and

$$g(t, \delta, \boldsymbol{\zeta}) = (|\dot{\psi}_d + \dot{\tilde{\psi}}| + 2\Gamma_1 + 2\Gamma_2)\delta + \Gamma_1(|\boldsymbol{\zeta}|, t) \quad (38)$$

Obviously, u_δ is UGB while it can be seen as an external input for the system (37). The unforced system (37), i.e. when $u_\delta = 0$, is a cascade connection of two GES systems with $g(t, \delta, \boldsymbol{\zeta})$ as the coupling term. According to [20], the

cascaded system made up of two UGES systems is UGES if the coupling term fulfills the linear growth rate condition which states there exist continuous functions $\beta_1, \beta_2 : \mathbb{R}_+ \to \mathbb{R}$ such that $\|g(t, \delta, \boldsymbol{\zeta})\| \le \beta_1(\|\boldsymbol{\zeta}\|) + \beta_2(\|\boldsymbol{\zeta}\|)|\delta|$. The functions β_1, β_2 may be constructed by a look at (38). Therefore, the unforced system (37) is UGES at the origin. The system is furthermore globally Lipschitz w.r.t $([\delta, \boldsymbol{\zeta}], u_\delta)$ uniformly in t. Consequently, the system (37) is input-to-state stable (ISS) [21] from u_δ to δ, and there exists a positive $c > 0$ such that $|\delta| \le c < \infty$. According to the comparison lemma [21], one concludes $\sigma \le \delta$. It follows that $|v_d| \le \sqrt{2c}$. That is, the ordinary differential equation (34) describes a globally bounded signal v_d, to which the unactuated dynamics converges. It also implies that the control forces are UGB and the control system is internally stable.

REFERENCES

[1] E. Lefeber, K. Pettersen, and H. Nijmeijer, "Tracking control of an underactuated ship," *Cont. Sys. Tech., IEEE Trans. on*, vol. 11, no. 1, pp. 52 – 61, 2003.

[2] A. P. Aguiar, J. P. Hespanha, and P. V. Kokotovic, "Path-following for nonminimum phase systems removes performance limitations," *Automatic Cont., IEEE Trans.*, vol. 50, no. 2, pp. 234–239, 2005.

[3] K. Y. Pettersen and H. Nijmeijer, "Underactuated ship tracking control: theory and experiments," *Int. J. of Cont.*, vol. 74, pp. 1435 – 1446, 2001.

[4] L. E. Dubins, "On curves of minimal length with a constraint on average curvature, and with prescribed initial and terminal positions and tangents," *American J. of Math.*, vol. 79, no. 3, pp. 497–516, 1957.

[5] T. I. Fossen, *Handbook of marine craft, hydrodynamics, and motion control*. John Wiley & Sons Ltd., 2011.

[6] K. Wichlund, O. Srdalen, and O. Egeland, "Control of vehicles with second-order nonholonomic constraints: Underactuated vehicles," in *ECC*, 1995.

[7] T.-J. Tarn, M. Zhang, and A. Serrani, "New integrability conditions for classifying holonomic and nonholonomic systems," in *Math. Sys. Theory and Optimization*, vol. 286, pp. 317–331, Springer, 2003.

[8] K. Pettersen and O. Egeland, "Exponential stabilization of an underactuated surface vessel," in *CDC*, vol. 1, pp. 967 –972 vol.1, dec 1996.

[9] E. Børhaug, A. Pavlov, E. Panteley, and K. Y. Pettersen, "Straight line path following for formations of underactuated marine surface vessels," *Cont. Sys. Tech., IEEE Trans. on*, vol. PP, no. 99, pp. 1–14, 2010.

[10] K. Pettersen and E. Lefeber, "Way-point tracking control of ships," in *CDC*, vol. 1, pp. 940 –945 vol.1, 2001.

[11] E. Fredriksen and K. Pettersen, "Global [kappa]-exponential way-point maneuvering of ships: Theory and experiments," *Automatica*, vol. 42, no. 4, pp. 677 – 687, 2006.

[12] K. D. Do, J. Pan, and Z. P. Jiang, "Robust adaptive control of underactuated ships on a linear course with comfort," *Ocean Engineering*, vol. 30, no. 17, pp. 2201 – 2225, 2003.

[13] T. I. Fossen, M. Breivik, and R. Skjetne, "Line-of-sight path following of underactuated marine craft," in *IFAC MCMC*, pp. 244–249, 2003.

[14] M. Breivik and T. I. Fossen, "Path following of straight lines and circles for marine surface vessels," in *IFAC CAMS*, pp. 65–70, 2004.

[15] I. A. F. Ihle, J. Jouffroy, and T. I. Fossen, "Formation control of marine surface craft: A lagrangian approach," *Oceanic Engineering, IEEE Journal of*, vol. 31, no. 4, pp. 922–934, 2006.

[16] C. Lanczos, *The variational principles of mechanics*. 4th ed., 1986.

[17] M. R. Flannery, "The enigma of nonholonomic constraints," *American Journal of Physics*, vol. 73, no. 3, pp. 265–272, 2005.

[18] X. Yun and N. Sarkar, "Unified formulation of robotic systems with holonomic and nonholonomic constraints," *Robot. & Auto., IEEE Trans. on*, vol. 14, pp. 640 –650, 1998.

[19] R. Skjetne, T. I. Fossen, and P. V. Kokotovic, "Robust output maneuvering for a class of nonlinear systems," *Automatica*, vol. 40, no. 3, pp. 373–383, 2004.

[20] A. Loria and E. Panteley, "Cascaded nonlinear time-varying systems: Analysis and design," , vol. 311 of *Lect. Notes in Cont. & Info. Sci.*, pp. 579–579, Springer, 2005.

[21] H. K. Khalil, *Nonlinear systems*. Prentice Hall, 3rd ed., 2002.